

## REDSHIFT $z \sim 1$ FIELD GALAXIES OBSERVED WITH THE KECK TELESCOPE AND THE *HUBBLE SPACE TELESCOPE*<sup>1,2</sup>

DAVID C. KOO, NICOLE P. VOGT, ANDREW C. PHILLIPS, RAFAEL GUZMÁN, K. L. WU,  
 S. M. FABER, CARYL GRONWALL, DUNCAN A. FORBES,  
 AND GARTH D. ILLINGWORTH

University of California Observatories/Lick Observatory, Board of Studies in Astronomy and Astrophysics,  
 University of California, Santa Cruz, CA 95064

EDWARD J. GROTH

Department of Physics, Princeton University, Princeton, NJ 08544

MARC DAVIS

Department of Astronomy, University of California, Berkeley, CA 94720

RICHARD G. KRON

Fermi National Accelerator Laboratory, MS 127, Box 500, Batavia, IL 60510

AND

ALEXANDER S. SZALAY

Department of Physics and Astronomy, The Johns Hopkins University, Baltimore, MD 21218

Received 1995 November 13; accepted 1996 April 23

### ABSTRACT

We report results based on 35 new spectroscopic redshifts obtained with the Keck Telescope for field galaxies that also have photometry and morphology from survey images taken by the refurbished *Hubble Space Telescope*. A sample of 24 redshifts for galaxies fainter than  $I = 22$  has a median redshift of  $z \sim 0.81$ . This result is inconsistent with the lower median redshift of  $z \sim 0.6$  predicted by the “maximal merger models” of Carlberg, which otherwise fit existing data. The data match an extrapolation of the Canada France Redshift Survey (CFRS), as well as predictions of certain mild luminosity-evolution models. Nearly half of the redshifts lie in two structures at  $z \simeq 0.81$  and  $z \simeq 1.0$ , showing the presence of high-density concentrations spanning scales of  $\sim 1 h^{-1}$  Mpc, i.e., the size of groups. We find emission lines or the presence of possible neighbors in seven of nine otherwise luminous galaxies with red central regions at redshifts beyond  $z \sim 0.7$ . We also note a diversity of morphological types among blue galaxies at  $z \sim 1$ , including small compact galaxies, “chains,” and “blue nucleated galaxies.” These morphologies are found among local, but generally less luminous, galaxies. Distant blue galaxies also include apparently normal late-type spirals. These findings could imply modest bursts of star formation caused by mergers or interactions of small, gas-rich galaxies with each other or with larger, well-formed galaxies. This first glimpse of very faint  $z \sim 1$  field galaxies of diverse colors and morphologies suggests that a mixture of physical processes is at work in the formation and evolution of faint field galaxies.

*Subject headings:* cosmology: observations — galaxies: distances and redshifts — galaxies: evolution — galaxies: formation — galaxies: structure

### 1. INTRODUCTION

To date, we have yet to understand the origin of the large density of very faint, blue field galaxies despite enormous observational progress (e.g., Lilly et al. 1995a). Deep images to  $I \sim 24$  or fainter with the refurbished *Hubble Space Telescope* (*HST*) show a predominance of late-type or unusual galaxy morphologies (e.g., Griffiths et al. 1994; Forbes et al. 1994; Glazebrook et al. 1995b; Driver et al. 1995), as well as small sizes that suggest a large fraction of low-luminosity dwarf galaxies (Driver et al. 1995). The redshifts of individual galaxies observed with *HST* remain largely unknown. Existing redshift samples include 17 galaxies to  $I \leq 22$  from Forbes et al. (1996), 32 to  $I \leq 22$  from Schade et al. (1995),

and 34 to  $B \leq 24.5$  (roughly  $I \leq 22.5$ ) from Cowie, Hu, & Songaila (1995) but do not yet probe fainter than  $I \sim 22$ . The redshift distribution is, however, well established statistically to  $I \leq 22$  from the CFRS (Lilly et al. 1995b). Redshifts are crucial for determining the intrinsic properties of galaxies visible in deep *HST* images, and good spectra can also yield rotation velocities, velocity dispersions, stellar population age indices, and metallicities. A program to obtain deep spectra using the 10 m Keck Telescope is now underway as a new initiative called the Deep Extragalactic Evolutionary Probe, or DEEP (Mould 1993; Koo 1995).

This paper reports on initial results of a new DEEP survey that utilizes redshifts from the Keck Telescope, supplemented by photometry, colors, and morphologies from images taken by Groth et al. (1996) with the refurbished *HST*. The target sample contains 230 galaxies, but poor weather permitted only 18% to be observed during the run. The acquired redshift sample of 35 galaxies is, however, generally representative of the target sample. The magnitudes are so faint (median  $I \gtrsim 22$ ; median  $B \sim 25$ ) and the

<sup>1</sup> Based on observations obtained at the W. M. Keck Observatory, which is operated jointly by the California Institute of Technology and the University of California.

<sup>2</sup> Based on observations with the NASA/ESA *Hubble Space Telescope*, obtained at the Space Telescope Science Institute, which is operated by AURA, Inc., under NASA contract NAS 5-26555.

redshifts so high (median  $z \sim 0.8$ ), that the current data provide a first glimpse of the nature of faint, distant field galaxies of  $\sim L^*$  luminosities at an epoch of roughly half the Hubble age.<sup>3</sup>

## 2. OBSERVATIONS

The *HST* data are from two surveys which we dub the “Survey Strip” taken under *HST* program GTO 5090 (E. Groth as principal investigator) and the “Deep Field,” under GTO 5109 (J. Westphal as principal investigator). The Survey Strip consists of 28 overlapping subfields taken with the *HST* Wide Field and Planetary Camera (WFPC2) and forms a “chevron strip” oriented NE to SW at roughly  $1417+52$  at Galactic latitude  $b \sim 60^\circ$ . Each of 27 subfields has exposures of 2800 s in the broad *V* filter (F606W) and 4400 s in the broad *I* filter (F814W). The 28th field is the Deep Field (J2000  $1417.5+52.5$ ), with total exposures of 24,400 s in *V* and 25,200 s in *I*. Astrometry and photometry of the entire Survey Strip has been completed, with full details of the survey, data reductions, and calibrations described by Groth et al. (1996). For the purposes of this paper, magnitudes are “total,” while (*V*–*I*) colors are based on 1" diameter apertures.

The morphologies were visually classified into three simple groups: “O” group for objects that appear round or elliptical, centrally concentrated, smooth, and largely symmetrical with at most a very weak disk; “S” group for objects that have both a bulge and an apparent disk and/or spiral arms; and “\*” group for galaxies that are likely to have on-going star formation with late-type, irregular, asymmetrical, multicomponent, or peculiar forms. These group designations were chosen to match the symbols used in the figures. Note that at redshifts  $z \sim 0.8$ , the *I* band corresponds to rest-frame *B*. Images of the entire spectroscopic sample are shown in Figures 1–2 (Plates 16–19) and 3 (Plate 20), along with magnitudes, colors, morphological group, redshifts (when known), and resulting absolute rest-frame *B* magnitudes and rest-frame (*U*–*B*) colors. Table 1 provides J2000 positions and corresponding identifications from CFRS.

Except for two bright (*I*  $\sim 18$ ) galaxies taken through clouds with a 1"0 wide long slit, the other 39 galaxy targets and several setup stars were observed through two focal-plane masks cut with multiple slitlets. This multislit mode allows simultaneous exposure of  $\sim 25$  or more targets with the Low Resolution Imaging Spectrograph (LRIS; see Oke et al. 1995). The detector was a Tektronix  $2048 \times 2048$  pixel CCD ( $24 \mu\text{m}$  or  $0".215$  pixel<sup>-1</sup>). With a slit width of  $1".23$ , a 600 lines mm<sup>-1</sup> grating yielded  $1.26 \text{ \AA pixel}^{-1}$  and an instrumental resolution of  $\sim 4 \text{ \AA FWHM}$ , i.e.,  $R \sim 2000$ . The spectral range was about 6500–9100 Å, depending on the exact position of the target on the mask. This spectral range was chosen to detect the strongest emission lines in faint galaxies:  $\text{H}\alpha$   $\lambda 6563$  at  $z \lesssim 0.4$ ,  $\text{H}\beta$   $\lambda 4861$  and  $[\text{O III}] \lambda 5007$  at  $0.3 \lesssim z \lesssim 0.8$ , and  $[\text{O II}] \lambda 3727$  at  $0.75 \lesssim z \lesssim 1.4$ . The slitlets were aligned along the 7" long axis of the LRIS field, which in turn was aligned with the NE-SW orientation

of the Survey Strip. Of the four allotted nights, only part of one night, UT 1995 May 1, was clear and calm enough to open the dome, during which we acquired  $4 \times 1800$  s exposures through one mask and  $3 \times 1800$  s through another at the same position (but with a different selection of galaxies). Seeing was variable but was estimated to be about  $0".8$  to  $1".2$  FWHM during most of the exposures. The spectroscopic reduction included the usual corrections for bias, dark, flats, and cosmic rays as well as skyline wavelength calibrations and background sky subtraction. We chose to place the targets at two positions along the slit, separated by 3", during different exposures. This “dither” allowed corrections for the 1%–2% fringing of the night sky seen at wavelengths greater than  $\sim 7200 \text{ \AA}$  by subtraction of the dithered images taken at each position. This method increases random sky noise by a factor of  $2^{1/2}$ .

The 230 galaxies chosen for spectroscopy, of which only 38 were actually observed with Keck, do not constitute a totally random, magnitude-limited sample. Rather, they were chosen to span the full distribution of colors and diverse visual morphologies of the galaxies in the whole Survey Strip. The field of our Keck observations included the Deep Field, where faint galaxies [ $24 \leq (V+I)/2 < 25$ ] were selected, and four adjacent WFPC2 subfields, where brighter targets [ $(V+I)/2 < 24$ ] were selected (see Fig. 4). As indicated in Table 1, a few special targets were chosen because of their unusual morphology (e.g., a promising quadruple-lens candidate); their detection in the radio; or their elongation with position angles promising for rotation curve measures (Vogt et al. 1996). In addition, redshifts were measured for four emission-line objects serendipitously

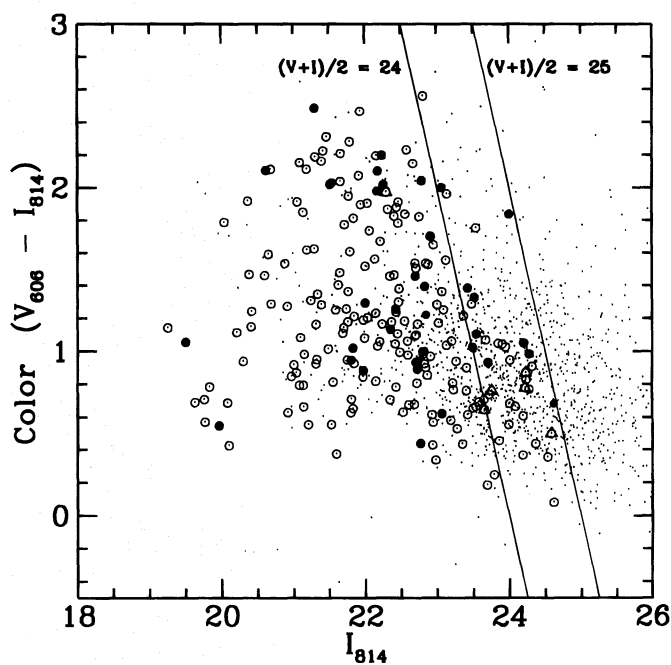


FIG. 4.—(*V*–*I*) vs. *I* plot showing a complete sample of objects found within fields 4 to 10 of the Survey Strip (dots); those chosen as the original Keck targets (circled dots); those for which Keck spectra and redshifts were actually acquired (solid circle); and those with Keck spectra but no redshifts (triangles). The two lines [ $(V+I)/2 = 24$ ,  $(V+I)/2 = 25$ ] mark the primary selection criteria for objects in the Deep Field; brighter targets were selected from the surrounding fields with the constraint  $(V+I)/2 < 24$ .

<sup>3</sup> We adopt  $h = 0.75$ ,  $q_0 = 0$ , and  $\Lambda = 0$ , i.e.,  $\Omega = 0$ . At redshift  $z \sim 1$ ,  $I \sim 22.6$  for a blue ( $B-V \sim 0.65$ ) galaxy of  $M_B \sim -20.4$  ( $M^*$ ), the look-back time is about 6.5 Gyr for a Hubble age of 13 Gyr, and 1" corresponds to 7 kpc.

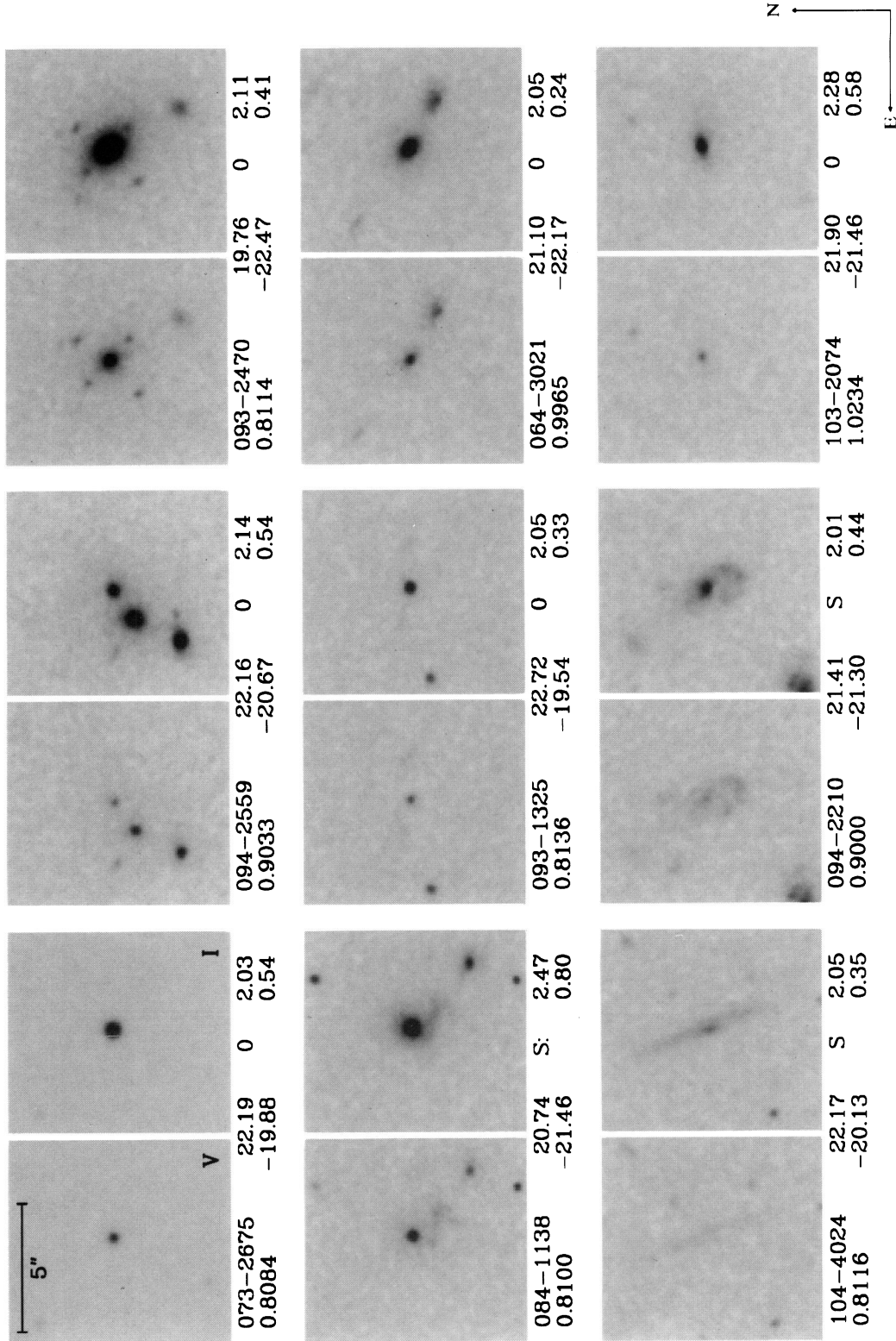


FIG. 1.—Distant Keck spectroscopic targets with red colors ( $V_{606} - I_{814} > 1.75$ ) within the central  $1''$  diameter and with high redshifts,  $z > 0.75$ . Each image ( $V_{606}$  on left and  $I_{814}$  on right) covers  $8'' \times 9''$  (unless cut off by the edge of WFPC2) and is the result of Hanning smoothing of the original. Each image pair is labeled by (first line) source identification number (see Table 1), total  $I$  mag, visual morphology group (0, S, or \*) as discussed in the text, observed ( $V - I$ ) color, then (second line) redshift followed by absolute luminosity ( $M_B$ ) and approximate rest-frame ( $U - B$ ) color. Highly uncertain values are marked with a colon. The cardinal directions are shown in the lower right-hand corner, and the image scale is marked in the upper left-hand corner.

KOO et al. (see 469, 536)

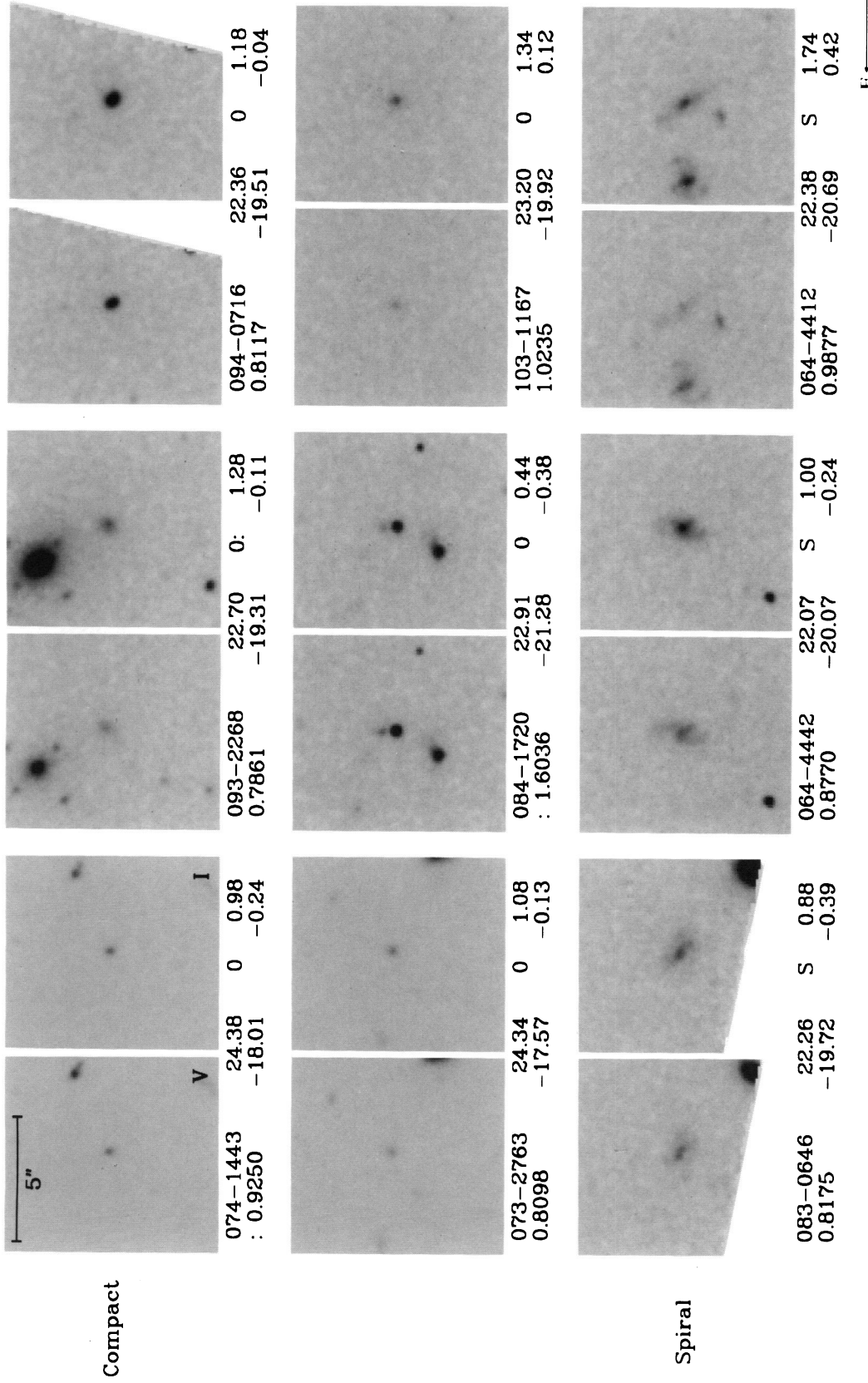


FIG. 2.—Similar to Fig. 1, but showing high-redshift targets with blue colors ( $V_{606} - I_{814} < 1.75$ ) or galaxies with no redshifts. The first set of blue, high-redshift galaxies (rows 1-7) is grouped roughly by similar morphology as follows. Row 1: very compact galaxies. Row 2: slightly more diffuse but still compact. Row 3: spirals. Row 4: possible spirals. Rows 5 and 6: diffuse galaxies with multiple knots of star formation that might be similar to the "blue nucleated galaxy" class proposed by Schade et al. (1995). Row 7: elongated diffuse galaxies that are similar to the "chain" class identified by Cowie et al. (1995). The second set of six targets (in rows 8 and 9) have no redshifts. As discussed in the text, we believe the one very red, relatively bright galaxy and five blue galaxies all belong to the high-redshift group.

KOO et al. (see 469, 536)

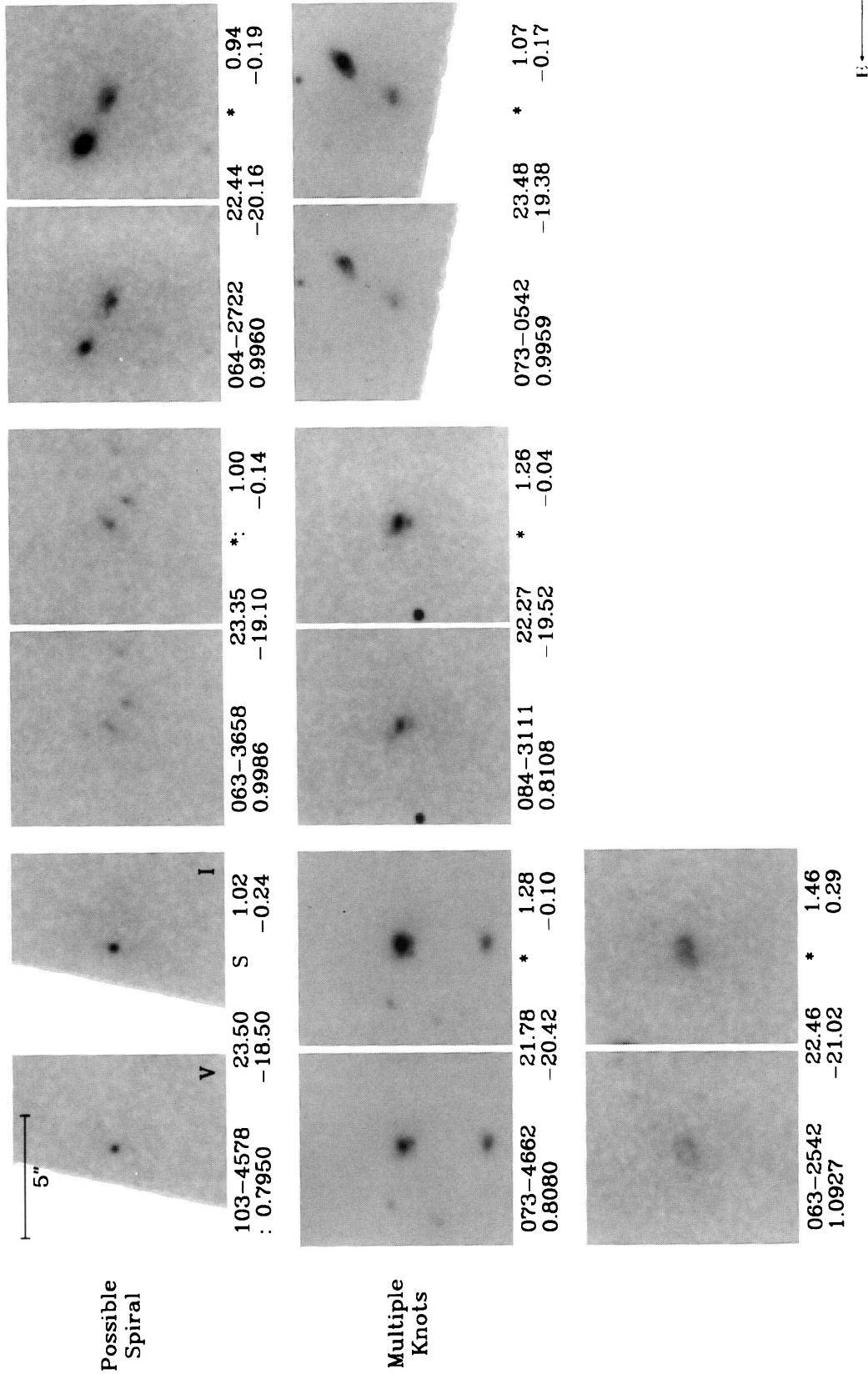


FIG. 2.—Continued

Koo et al. (see 469, 536)

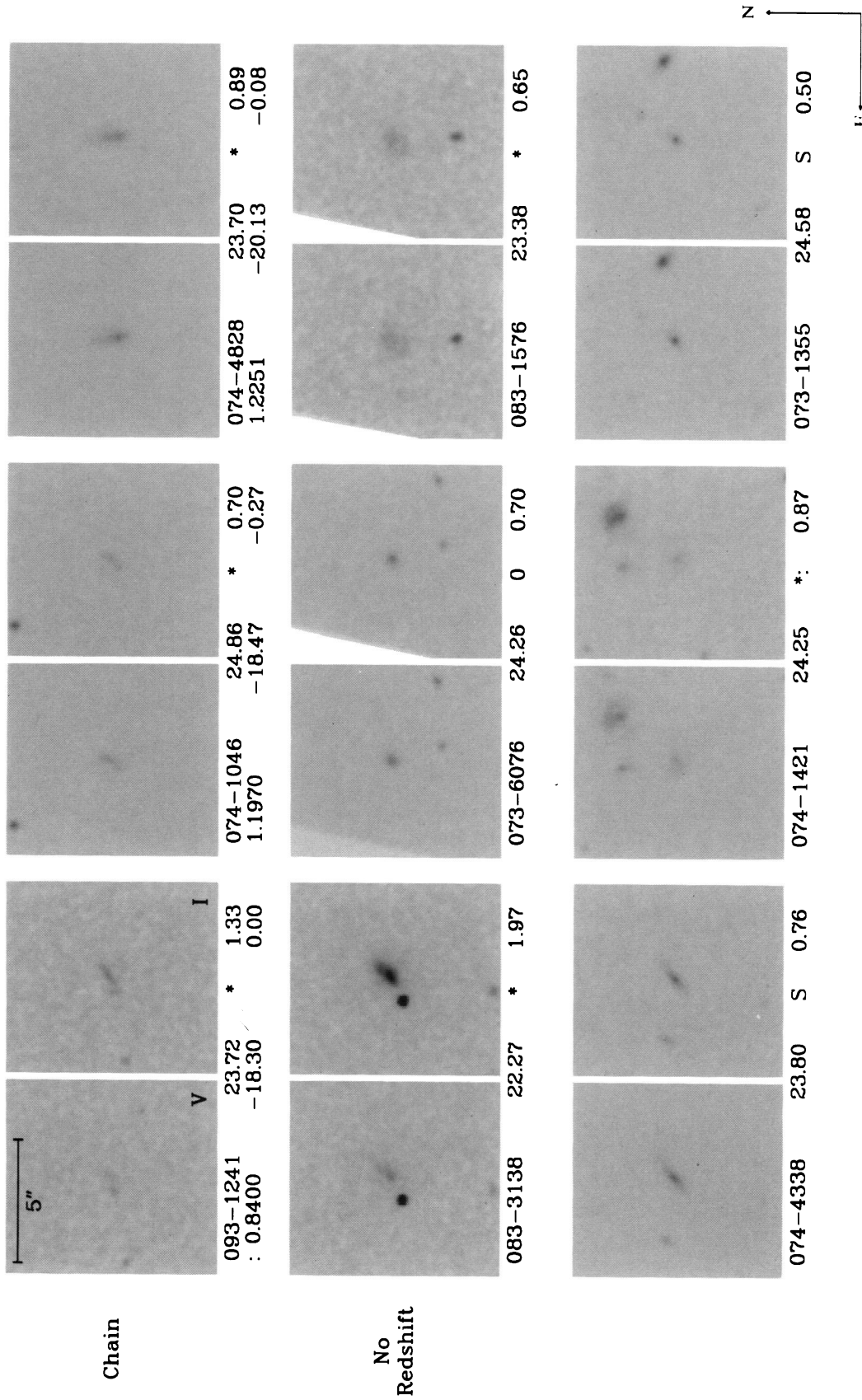


Fig. 2.—Continued

Koo et al. (see 469, 536)

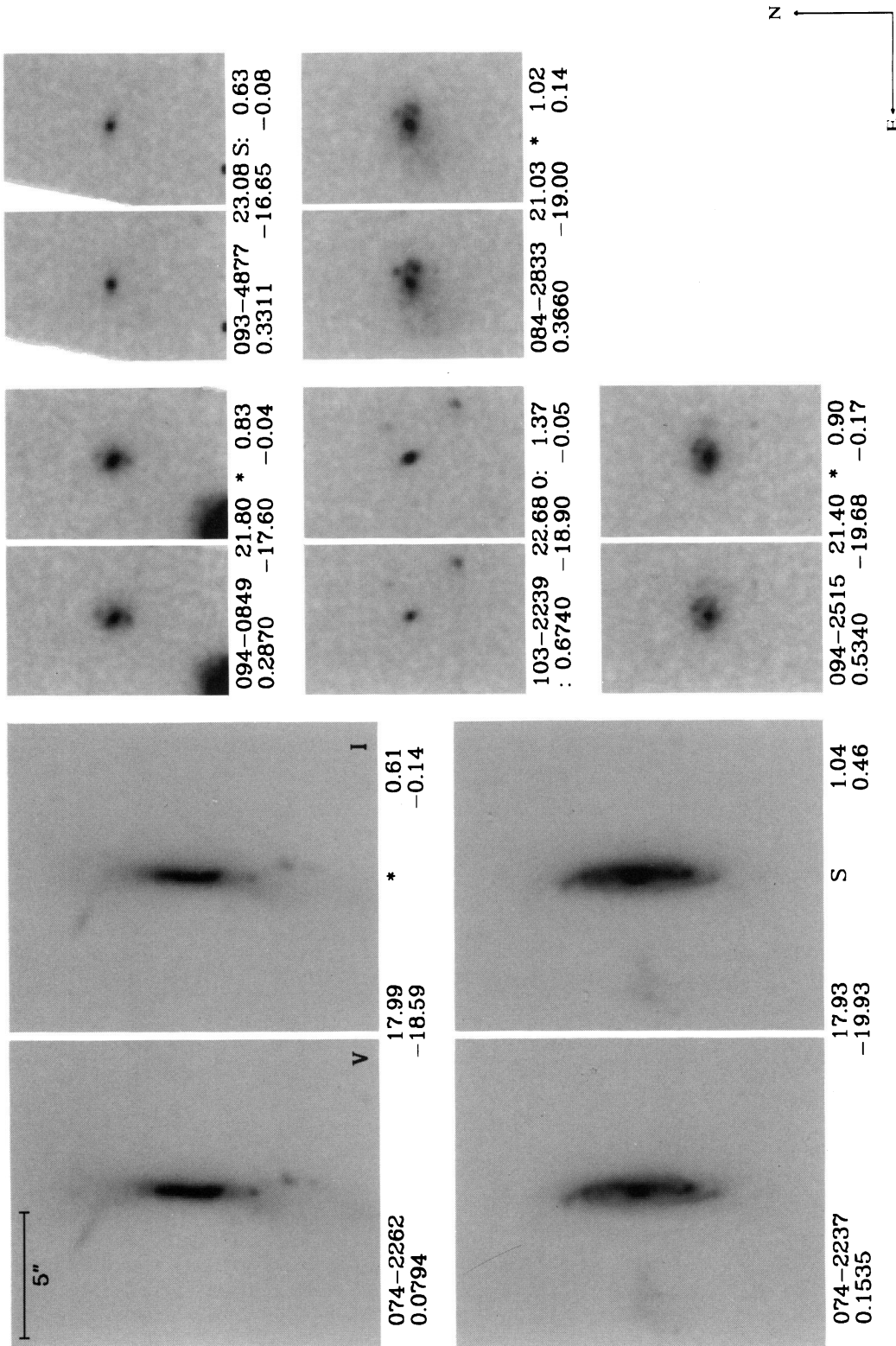


FIG. 3.—Similar to Figs. 1 and 2, but for lower redshift galaxies ( $z < 0.75$ ). The images of the two galaxies at a redshift lower than 0.2 are  $12''.5 \times 15''$ , and those of the five galaxies with redshifts between 0.2 and 0.75 are  $5'' \times 9''$ .

KOO et al. (see 469, 536)

TABLE 1  
OBSERVED GALAXY DATA

Number (1)	Source ID (2)	R.A. (3)	Declination (4)	Observed $z$ (5)	$I_{\text{tot}}$ (6)	Morphology (7)	Panel Class (8)	Comments (9)
1	103-2239	14 17 25.93	52 25 26.87	0.6740:	22.68	0	Intermediate $z$	
2	104-4024	14 17 27.00	52 24 50.94	0.8116*	22.17	S	Red	Rotation curve candidate
3	103-1167	14 17 29.19	52 25 22.02	1.0235*	23.20	0	Compact	
4	103-4578	14 17 29.61	52 25 58.08	0.7950:	23.50	S	Possible spiral	Serendipitous
5	103-2074	14 17 29.70	52 25 32.54	1.0234	21.90	0	Red	
6	094-0716	14 17 29.84	52 26 01.25	0.8117	22.36	0	Compact	
7	094-0849	14 17 30.68	52 25 28.93	0.2870	21.80	*	Intermediate $z$	
8	093-1325	14 17 31.18	52 26 25.24	0.8136	22.72	0	Red	
9	094-2210	14 17 31.31	52 26 08.81	0.9000	21.41	S	Red	
10	094-2515	14 17 31.75	52 26 05.47	0.5340	21.40	*	Intermediate $z$	(14.1395; 0.5301)
11	094-2559	14 17 32.75	52 25 22.61	0.9033	22.16	0	Red	
12	093-1241	14 17 33.00	52 26 27.51	0.84:	23.72	*	Chain	
13	093-2268	14 17 35.58	52 26 42.77	0.7861	22.70	0	Compact	Serendipitous
14	093-2470	14 17 35.74	52 26 45.67	0.8114	19.76	0	Red	Lens candidate <sup>a</sup> ; (14.1311; 0.8065)
15	093-4877	14 17 35.93	52 27 09.55	0.3311	23.08	S	Intermediate $z$	
16	084-1138	14 17 37.26	52 26 49.66	0.8100	20.74	S	Compact	(14.1277; 0.8100)
17	084-1720	14 17 37.50	52 27 08.89	1.6036:	22.91	0	Compact	Fe II $\lambda$ 2600 in absorption
18	083-3138	14 17 38.78	52 27 55.06	...	22.27	*	No $z$	15V15 <sup>b</sup>
19	084-3111	14 17 38.85	52 27 20.79	0.8108	22.27	*	Multiple knots	
20	084-2833	14 17 39.02	52 26 57.72	0.3660	21.03	*	Intermediate $z$	(14.1239; 0.3616)
21	083-0646	14 17 40.14	52 27 32.25	0.8175	22.26	S	Spiral	
22	083-1576	14 17 43.14	52 27 47.78	...	23.38	*	No $z$	
23	074-1421	14 17 43.86	52 28 16.12	...	24.25	*	No $z$	
24	074-1046	14 17 44.02	52 27 50.69	1.1970*	24.86	*	Chain	Serendipitous
25	074-1443	14 17 44.30	52 27 54.87	0.9250:	24.38	0	Compact	
26	074-2237	14 17 45.06	52 28 02.47	0.1535	17.93	S	Intermediate $z$	Long slit; (14.9025; 0.1550)
27	074-2262	14 17 45.61	52 27 37.89	0.0794	17.99	*	Intermediate $z$	Long slit; (14.1039; 0.0793)
28	073-0542	14 17 46.41	52 28 39.65	0.9959*	23.48	*	Multiple knots	
29	074-4338	14 17 47.29	52 28 05.78	...	23.80	S	No $z$	
30	073-4662	14 17 47.52	52 29 24.23	0.8080	21.78	*	Multiple knots	(14.0985; 0.8073)
31	074-4828	14 17 47.58	52 28 15.84	1.2251*	23.70	*	Chain	
32	073-1355	14 17 47.59	52 28 50.57	...	24.58	S	No $z$	
33	073-2763	14 17 48.07	52 29 05.85	0.8098*	24.34	0	Compact	
34	073-6076	14 17 48.74	52 29 39.96	...	24.26	0	No $z$	
35	073-2675	14 17 49.32	52 29 07.54	0.8084	22.19	0	Red	
36	064-2722	14 17 51.82	52 29 28.36	0.9960*	22.44	*	Possible spiral	Serendipitous
37	064-3021	14 17 52.03	52 29 29.33	0.9965	21.10	0	Red	15V39 <sup>b</sup> ; (14.0854; 0.9920)
38	063-2542	14 17 52.51	52 30 08.79	1.0927*	22.46	*	Multiple knots	
39	064-4412	14 17 53.42	52 29 41.08	0.9877*	22.38	S	Spiral	
40	063-3658	14 17 53.91	52 30 23.03	0.9986*	23.35	*	Possible spiral	
41	064-4442	14 17 54.04	52 29 11.29	0.8770	22.07	S	Spiral	

NOTES.—Col. (1): Sequence number ordered by right ascension. Col. (2): Source identification number is given by FFC-XXYY, where FF is the subfield, C is the WFPC2 chip number, and XX and YY are the chip coordinates in units of 10 pixels. Cols. (3) and (4): J2000 coordinates from Groth et al. 1996; right ascension in hours, minutes, and seconds; declination in degrees, arcminutes, and arcseconds. Col. (5): Keck redshifts; a semicolon means highly uncertain, an asterisk means probable, with the remainder being very probable to secure. Col. (6): Total  $I_{814}$  magnitude. Col. (7): Morphology as described in § 2; also used in Figs. 1, 2, 3, and 6. Col. (8): Divisions used for organizing Fig. 1 (high  $z$  red galaxies), Fig. 2 (high  $z$  blue galaxies: spiral, possible spiral, compact, multiple knots, chains, and no  $z$ ), and Fig. 3 (intermediate  $z$ ). Col. (9): Comments with (ID;  $z$ ) are from CFRS (Lilly et al. 1995a).

<sup>a</sup> Possible quad lens candidate (Ratnatunga et al. 1995; Broadhurst et al. 1996; Crampton et al. 1996).

<sup>b</sup> Radio source from Fomalont et al. 1991.

lying within slitlets of intended targets. The faintest objects were observed through both masks. Within small number statistics and as shown in Figure 4, the present Keck sample has a color distribution at each magnitude roughly similar to the entire *HST* sample, except that 10 galaxies (rather than the expected seven) were observed with very red colors ( $V-I > 1.6$ ) and magnitudes  $20 < I < 23.25$ .

The redshift identifications were made by first visually inspecting the two-dimensional sky-subtracted images for any strong emission lines. The extracted one-dimensional spectra were then examined for absorption lines when the continuum was bright enough, generally for galaxies with  $I \lesssim 23$ , or weaker emission features. In total, we have extracted 24 redshifts for our original targets, four redshifts for objects fortuitously lying in a slitlet, and two redshifts from long-slit observations of  $I \sim 18$  galaxies. The reliability of these redshifts range from high (i.e., secure

redshifts) to moderately high (i.e., probable redshifts). In several galaxies, only one emission line was detected, but its identification as [O II]  $\lambda$ 3727 was considered to be secure if we resolved the doublet or found a rising continuum to the red. Five more objects have apparent emission or absorption features, but highly uncertain redshifts; six targets fainter than  $I \sim 22.3$  have yet to yield any reliable spectral features for redshift determination. Figure 5 shows examples of our Keck spectra that span a range of redshift reliability.

An independent check of our coordinates, photometry, and redshifts can be made from the eight galaxies in common with CFRS (see Table 1 and Lilly et al. 1995a) and shows good agreement. We find a mean positional offset between the CFRS and our coordinates of  $\sim 1''.1 \pm 0''.4$ , which is certainly close enough to make secure identifications. The mean  $I$ -band difference (CFRS  $I_{\text{AB}} - I_{\text{tot}}$ ) is

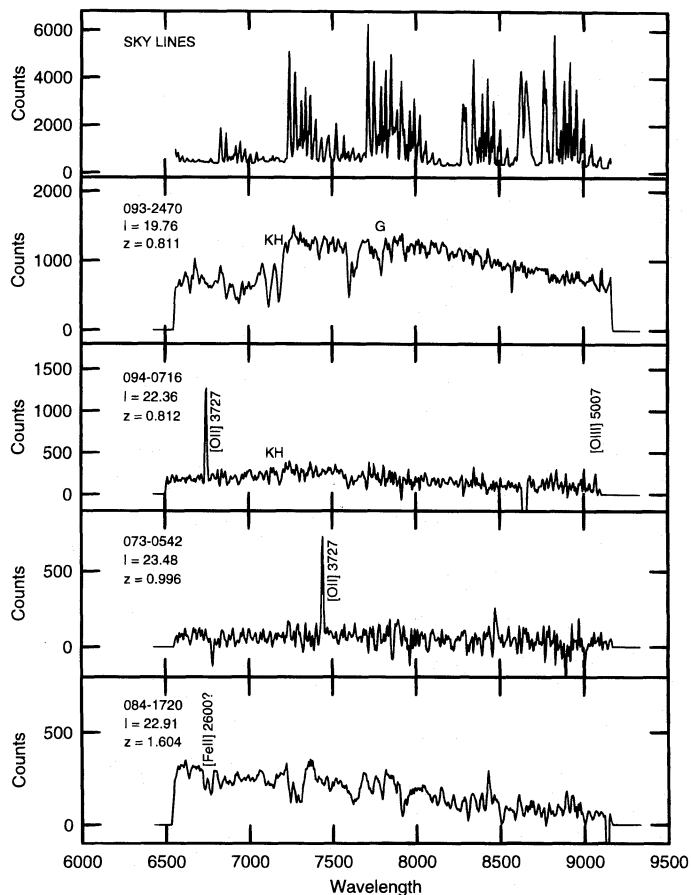


FIG. 5.—Counts vs. wavelength for sample Keck spectra, each labeled with the source name, total  $I_{814}$  mag, and redshift. The top one is for an 1800 s exposure of the night sky. The next two are galaxies whose redshifts are secure, with one being a bright galaxy with several strong absorption lines and the other being a 2.6 mag fainter galaxy with resolved [O II] emission lines and [O III]. The next galaxy is another magnitude fainter with an emission line that we identify as [O II], but since it has no other signatures to confirm this identification, its redshift reliability is only probable. The last galaxy is bright enough to yield definite absorption lines, but we feel the identification of these with Fe II is tentative, and thus highly uncertain, at this time. The strengths of the spectral features in these galaxy spectra, all with 2 hr exposures and smoothed with a 7 pixel boxcar (except for 084–1720, which was smoothed with a 15 pixel boxcar), are higher than average.

expected to be  $\sim 0.48$  mag, while we find  $0.56 \pm 0.33$ ; dropping the two very bright, large galaxies, 074–2237 and 074–2262, whose photometry might be difficult, yields a significantly smaller standard deviation ( $\pm 0.18$ ) and a mean within expectations (0.46 mag). Finally, the redshifts of all eight CFRS galaxies in common with our Keck sample agree well individually, but have slightly lower values than ours by a mean difference of  $\delta z = 0.0021 \pm 0.0025$  (see Table 1).

### 3. RESULTS

The Keck redshift survey is 100% complete for targeted objects to  $I \sim 22.3$  (24 galaxies) and 85% complete for the whole sample to  $I \lesssim 24.5$ . We reached beyond  $I \sim 23$  only for targets with strong emission lines; the redshifts of several of these faint galaxies remain highly uncertain (see Table 1). Figure 6b shows the magnitude versus redshift distribution of the sample, plus the 17 galaxies from Forbes et al. (1996).

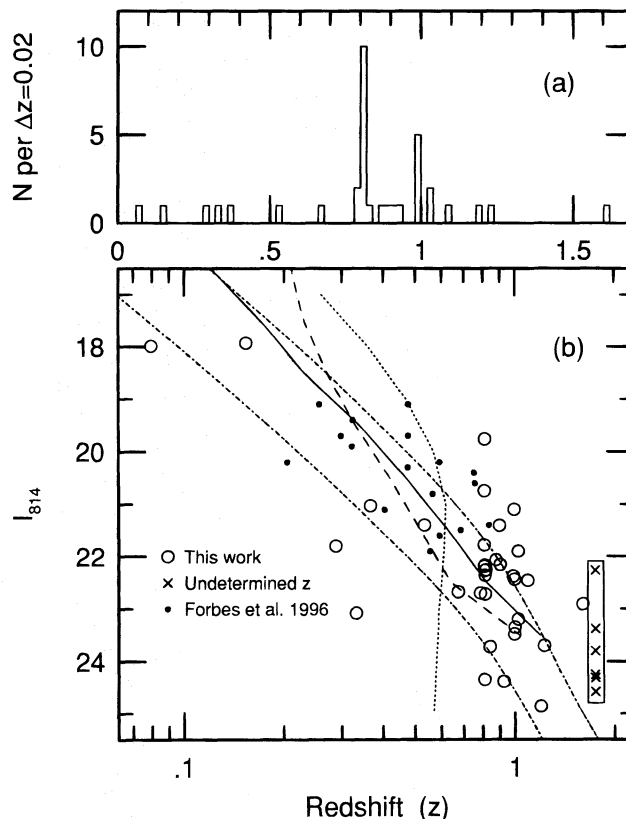


FIG. 6.—Upper panel (a) shows the redshift histogram for the Keck targets from this work in bins of 0.02 in  $z$ , while the lower panel (b) shows an  $I$  magnitude vs. redshift  $z$  (on a logarithmic scale) plot from this work, plus 17 galaxies from Forbes et al. (1996). For comparison to models, the solid line in (b) shows the median curve predicted from the evolving model of Gronwall & Koo (1995); the dashed line shows the median curve predicted from a standard no-evolution model (Guiderdoni & Rocca-Volmerange 1990). The dotted line shows the predicted median curve from the “maximal merger model” of Carlberg (1996). For discriminating the relative luminosities of the galaxies, the dash-dot lines have been included to show the track for an  $M^*$  and  $M^* + 2$  galaxy that has the color of an Sbc galaxy. Objects without redshifts are placed in the box at their respective magnitude positions.

The most striking aspect of the data is the high fraction of redshifts  $z \geq 0.8$ . The resultant median of the observed redshifts is 0.81. Due to the relatively high level of completeness, the median value of the whole sample must lie in the range 0.81 to 1.00, even if the undetermined redshifts are entirely at  $z < 0.6$  or at  $z > 1.4$ , or if the number of galaxies at the  $z = 0.81$  and 1.00 peaks are halved to account for small-scale clustering effects.

For comparison, the CFRS sample (Lilly et al. 1995a) has nearly 600 redshifts to  $I = 22$ , a median redshift of  $z \sim 0.56$ , an overall completeness of 85%, and completeness for  $21 < I < 22$  of 74%. Our sample is 100% complete to these limits and includes 25 redshifts beyond  $z \sim 0.8$ , more than the four such redshifts in the  $B \leq 24$  survey of Glazebrook et al. (1995a), the 13 in the  $K \leq 20$  survey of Songaila et al. (1994), or the five in the  $I \leq 22$  targets of Schade et al. (1995), but still far short of the  $\geq 150$  in the CFRS.

Figure 7 plots  $(V-I)$  color versus redshift for the Keck sample with morphological information encoded within the symbol shapes. The curves provide a guide to the intrinsic colors of local galaxies and to the expected colors for single instantaneous starbursts originating at redshifts  $z = 1$  or  $z = 2$ . One striking aspect of this figure is how well the

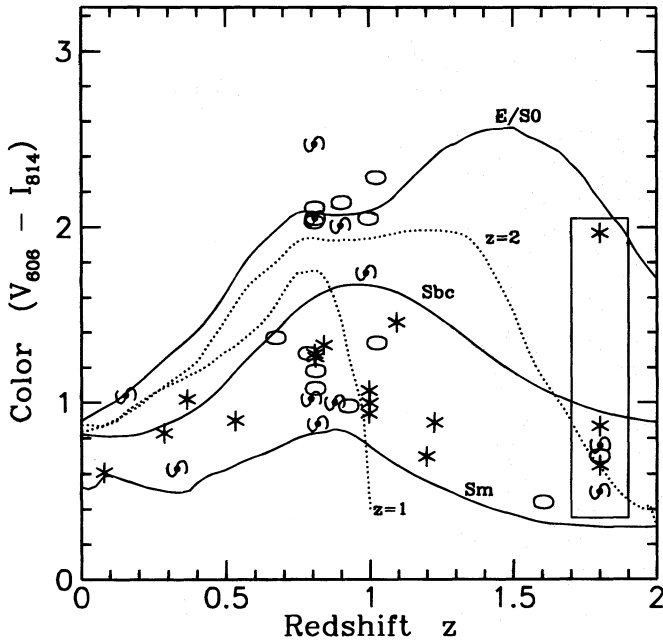


FIG. 7.— $(V-I)$  color vs. redshift for Keck targets from this work. Objects without redshifts are placed in the box to the right. Morphologies are indicated by symbols “O,” “S,” and asterisk that match the visual morphology groups discussed in the text. Several labeled lines show expected colors for various spectral energy distributions: (a) an instantaneous burst of star formation at redshift  $z \sim 2$  (using the models of Bruzual & Charlot 1993) that becomes almost as red as (b) a nonevolving local elliptical or S0 (E/S0) by  $z < 1$ ; (c) model burst at  $z = 1$  that might be compared to the bursting dwarfs in the fiducial model of Babul & Ferguson (1996); (d) a nonevolving local Sbc galaxy; and (e) the bluest one, derived from a nonevolving spectrum of NGC 4449, a nearby, very actively star-forming Sm galaxy.

galaxies fall within the bounds seen in local galaxies, a result already found in the larger CFRS sample (Crampton et al. 1995). We find no evidence for a significant new population of unusually blue or unusually red galaxies.

Other straightforward results are that very red *field* galaxies do exist at high redshifts ( $z \gtrsim 0.7$ ) and that such galaxies have colors comparable to those found for local ellipticals; therefore, their most recent major star formation event presumably occurred at redshifts  $z \gtrsim 2$ . Moreover, the intrinsically reddest galaxies are not necessarily purely elliptical in morphology; bulges and at least one dust-reddened, inclined spiral are seen. Although low-clustering amplitudes have been measured in angular correlation studies (e.g., Efstathiou et al. 1991), the intrinsically blue galaxies here do partake in the strong clustering seen at redshifts  $z \sim 0.8$  and 1.0. They may thus contribute to the strong angular clustering observed among the bluest galaxies by Landy, Szalay, & Koo (1996). The diverse morphologies of these high-redshift, clustered galaxies are easily seen in Figures 1 and 2.

## 4. DISCUSSION

### 4.1. Redshift Distribution

What cosmological implications can we extract from this faint sample of galaxies? Given the relatively small numbers, median redshifts are a good starting point for comparison to theory. First, the 100% complete sample of nine galaxies with  $19.5 < I < 22$  has a median redshift of  $z = 0.81$ , with a possible range of 0.37 to 1.00 at the 95% confidence level; this is consistent with the median of 0.56

for CFRS based on a much larger sample. Second, the  $I \geq 22$  sample with 24 galaxies has the same median of 0.81 but a tighter range of  $z \sim 0.81$  to 1.00 at the 95% confidence level. This high median is an important finding, since Songaila et al. (1994) found the median to remain at  $z \lesssim 0.6$  for galaxies fainter than  $K \sim 18$  (roughly  $I \sim 20.5$ ), as predicted by some merger models. For example, the “maximal merger model” of Carlberg (1996), which matches observations to  $I \sim 22$ , predicts that the median will stabilize at  $z \sim 0.6$  from  $I \sim 20$  all the way to  $I \sim 28$ , contrary to what we find in this sample at  $I > 22$ . The high median is, however, consistent with at least two other scenarios. First, with no further evolution than that already found in the CFRS survey, Lilly et al. (1995c) predict that the median should continue to rise to  $z \sim 0.9$  for  $22 < I < 23$  and to  $z \gtrsim 1.0$  for  $23 < I < 24$ . Second, the predictions of models that do include mild luminosity evolution but no mergers, such as those of Gronwall & Koo (1995), are virtually identical to those predicted by CFRS. At this time, we have no basis to exclude other models, such as those of Cole et al. (1994), that analytically track various other physical processes such as supernova gas removal and star formation, as well as merging of dark matter halos.

The width of the distribution is also a potentially powerful discriminant. For example, the fiducial bursting dwarf model of Babul & Ferguson (1996) predicts a narrow redshift distribution peaked at  $z \lesssim 1$  for a  $B < 26$  redshift sample, with a cutoff in numbers at  $z = 1$ , chosen by them by fiat, when dwarfs first form. Our data, with the bulk of the redshifts  $0.7 \lesssim z \lesssim 1$ , lend some support for this picture. On the other hand, several very blue galaxies are seen beyond  $z = 1$ , while those very near  $z = 1$  span a wide range of colors rather than being dominated by the very blue colors expected from an ongoing burst of star formation (see Fig. 7). Moreover, the diverse morphologies and diffuseness of many of the blue galaxies, discussed below, may be difficult to explain. More faint redshifts with stricter selection criteria will be needed to provide more definitive tests of the bursting model.

Redshifts also probe clustering. CFRS already paved the way with the discovery of 12 redshifts in a 0.016 redshift interval, indicating a 5–10 times overdensity of galaxies at  $z = 0.985$  (Le Fèvre et al. 1994). This possible supercluster structure was found in a  $10' \times 10'$  field that coincidentally overlaps our field. As seen in Figure 6a, we find a density enhancement at  $z = 0.995 \pm 0.004$  containing five galaxies, which may be the same structure, plus another stronger one at  $z = 0.811 \pm 0.003$  with 10 galaxies (standard deviations are measured within  $\delta z = \pm 0.02$  of the peak). Since we see no visual evidence for any rich cluster of galaxies in our field and the velocity dispersion is relatively low ( $\sim 450 \text{ km s}^{-1}$ ), the  $z = 0.81$  enhancement is probably a rich group.

### 4.2. Morphologies, Colors, and Galaxy Evolution

We close with some discussion and speculations based on HST morphologies and colors. Figure 1 shows nine galaxies with very red colors within their central  $1''$  diameters. The galaxies in the top two rows of Figure 1 appear morphologically to be elliptical or S0 galaxies (although Phillips et al. [1996] find that 073–2675 is better fitted with an exponential, rather than an  $r^{1/4}$  profile). Combined with very red colors, these galaxies indicate the presence of luminous ellipticals in the field that are already quite old by  $z \sim 1$ . This presumes that the red colors are not due to dust

extinction, which remains to be determined. Based on the  $z = 2$  curve in Figure 7, the last significant star formation event presumably occurred at redshifts  $z \sim 2$  or greater. Such very red galaxies have also been found among distant radio galaxies (e.g., McCarthy 1993) and cluster galaxies (e.g., Dickinson 1996).

Yet several of these galaxies are not quite “normal.” Galaxy 093–2470 appears to have four very blue compact objects imbedded in a symmetrical pattern within its halo, a pattern proposed to form a “quad-lens” system (Ratnatunga et al. 1995; Broadhurst et al. 1996; Crampton et al. 1996). Although the “maximal merger model” of Carlberg (1996) appears to be invalidated by the new redshifts, we do find some evidence for minor mergers among several of these distant red galaxies. Except for 073–2675, the remaining five galaxies in the first two rows of Figure 1 show close projected neighbors or tidal and merger “tails,” and some of this neighboring material is blue. Perhaps we are watching the infall of dwarf galaxies, some possibly quite gas rich, if the blue colors are due to active star formation. The implication would be that elliptical galaxies form early and yet can be built up by minor mergers over a much longer time period. This scenario could reconcile the apparent lack of luminosity or density evolution among red galaxies seen in the CFRS (Lilly et al. 1995c) or the Mg II absorber sample (Steidel, Dickinson, & Persson 1994) with the presence of well-formed, red field galaxies at an early epoch.

The last row of Figure 1 presents three very red *disk* galaxies. With a peak-to-peak rotation curve velocity of  $\sim 600 \text{ km s}^{-1}$  (Vogt et al. 1996), the conspicuous edge-on system (104–4024) demonstrates that some massive, thin-disk, dusty systems already exist at  $z \sim 0.8$ , roughly half a Hubble age ago. This single object, evidently similar to our Milky Way, supports what we believe to be the early formation of our own old disk. There are hints of very faint blue satellites that might eventually settle into this distant spiral, an evolutionary path that has also been proposed for the Milky Way (Majewski 1993).

Another disklike system, 094–2210, shows a very red, bulgelike core surrounded by numerous blue “blobs” or arms. If this galaxy is a disk or protodisk system with little dust extinction, it suggests that some bulges are already quite old by  $z \sim 1$ , with their most recent star formation occurring perhaps at  $z \gtrsim 2$  (see Fig. 7). Object 103–2074 appears to be another disky system of early type (S0 or Sa) with a very red bulge.

Figure 2 shows two sets of galaxies: the bluer, high-redshift galaxies and those without redshifts. Those with measured redshifts  $z \gtrsim 0.75$  are organized into seven rows divided into morphological groups. We argue that all six of the galaxies without redshifts are likely to be at high redshifts  $z \gtrsim 0.75$ . Since blue galaxies normally have strong emission lines of [O II]  $\lambda 3727$  that should be detectable to  $z \approx 1.4$  (or especially of H $\alpha$  for redshifts lower than  $z \sim 0.4$ ), we argue that the five blue galaxies in our Keck sample without measured redshifts are probably at higher redshifts. In support of this conjecture, we note that the bluest galaxy in our entire Keck sample (source 084–1720) has two definite absorption lines separated by  $\sim 35 \text{ \AA}$  and appearing around  $6770 \text{ \AA}$  (see Fig. 5); we tentatively identify this doublet as Fe II  $\lambda 2587$  and  $\lambda 2600$  that would yield a redshift of  $z = 1.60$ . One relatively bright, very red galaxy (source 083–3138) also has no redshift, but based on the similarity

of its color to the galaxies in Figure 1 with redshifts (see Fig. 7), we infer that it is likely to be at high redshift. The targets without redshifts are all presented in the last two rows of Figure 2.

The large diversity of morphologies displayed in Figure 2 is striking, ranging from compact galaxies shown in the first and second rows, normal disklike systems in the third and fourth rows, to irregular, late-type systems with multiple blue star formation sites in the fifth and sixth rows. This last group could be related to a proposed new class of “blue-nucleated” galaxies (Schade et al. 1995). The seventh row shows galaxies that are perhaps more elongated versions of the above galaxies or that may belong to the new class of “chain” galaxies defined by Cowie et al. (1995). Comparably complex and diverse morphologies can, however, be found even among local very blue galaxies such as clumpy irregulars, Markarian galaxies, extragalactic H II regions, merging galaxies, or other peculiar classes (c.f. images of H II galaxies presented by Melnick 1987). These various local blue systems often show similar, multiple concentrations of intense star formation.

The new Keck redshifts and *HST* morphologies combine to counter the view that low-redshift, very blue, low-luminosity dwarf galaxies dominate the late-type, peculiar systems detected in deep *HST* images (e.g., Driver et al. 1995). Instead, most of the Keck galaxies with these morphologies are at high redshifts and are thus relatively luminous, although typically less luminous than  $L^*$ . The apparent sizes of many of these distant galaxies are  $\sim 1''$ , however, which imply metric sizes of several kiloparsecs, quite typical of local dwarf galaxies. After corrections for cosmological dimming (about 2.3 mag at  $z \sim 1$ ) and *K*-corrections (from  $\sim 0$  mag for very blue galaxies to over 4 mag for very red galaxies at  $z \sim 1$ ), the resultant rest-frame *B*-band surface brightnesses are higher than those of most local spirals and star-forming irregulars (Schade et al. 1995; Phillips et al. 1996). Thus, the faint blue galaxies are not explained by a class of very low surface brightness galaxies that have been missed by local surveys (McGaugh 1994). Whether the high-redshift galaxies are indeed low-mass systems (which may or may not have any direct relationship to local dwarfs) or are the luminous tips of more massive systems will be decided by results of kinematic surveys. So far, only small samples of very blue, distant, field galaxies have been observed, many quite compact and as distant as  $z \sim 0.8$ , and these have yielded some luminous galaxies with very low, emission-line velocity widths of  $\sigma \lesssim 70 \text{ km s}^{-1}$  (Koo et al. 1995; Colless 1995; Guzmán et al. 1996; Forbes et al. 1996).

We conclude from the present sample that no single physical process (e.g., mergers or bursting dwarfs) dominates the evolution of faint galaxies at redshifts  $z \sim 1$ . We find a diversity of morphologies from normal to peculiar, with no firm evidence for entirely new classes of galaxies for which local counterparts cannot be found, a conclusion also reached by Forbes et al. (1996). We also find bulge and elliptical systems that are well formed and red. Equally tantalizing are the hints that a large fraction of galaxies are participating in further agglomeration and continued star formation due to interactions, major mergers, and infalling satellites. Taken together, these early Keck results for distant *HST* galaxies imply that much larger samples will be needed to disentangle and understand this exciting, complex, and very important early history of galaxies.

We are grateful to the staff of the Keck Observatory, especially T. Bida, for their assistance, as well as J. Lewis at the UCO/Lick Observatory Laboratories for fabricating the masks. The Center for Particle Astrophysics initiated the DEEP program and continues to provide support. We also thank C. Steidel and R. Blandford for their comments and participation in DEEP and Jason Rhodes, Rick Balsano, and the WFPC-1 Investigation Definition Team for prepublication access to their catalog and *HST* images.

We are grateful to the referee for several useful suggestions. Funding for this work was provided by NSF grants AST 92-2540, AST 91-20005, and AST 88-58203; NASA grants AR-5801.01-94A, GO-2684.04-87A, GO-2684.05-87A, and WFPC-1 Investigation Definition Team Grants NAS 5-1661 and NAS 5-1629. R. G. acknowledges funding from the Spanish MEC fellowship EX93-27295297; C. G. from an NSF Graduate Fellowship.

## REFERENCES

- Babul, A., & Ferguson, H. C. 1996, *ApJ*, 458, 100  
 Broadhurst, T. J., et al. 1996, in preparation  
 Bruzual A. G., & Charlot, S. 1993, *ApJ*, 405, 538  
 Carlberg, R. G. 1996, in Proc. MPI Conf., *Galaxies in the Young Universe*, ed. H. Hippelein, K. Meisenheimer, & H. J. Röser (Berlin: Springer), 206  
 Cole, S., Aragon-Salamanca, A., Frenk, C. S., Navarro, J. F., & Zepf, S. E. 1994, *MNRAS*, 271, 781  
 Colless, M. 1995, in *Wide Field Spectroscopy and the Distant Universe*, ed. S. Maddox & A. Aragon-Salamanca (Singapore: World Scientific), 263  
 Cowie, L. L., Hu, E. M., & Songaila, A. 1995, *AJ*, 110, 1526  
 Crampton, D., Le Fèvre, O., Hammer, F., & Lilly, S. J. 1996, *A&A*, in press  
 Crampton, D., Le Fèvre, O., Lilly, S. J., & Hammer, F. 1995, *ApJ*, 455, 96  
 Dickinson, M. 1996, in ASP Conf. Ser. 86, *Fresh Views on Elliptical Galaxies*, ed. A. Buzzoni, A. Renzini, & A. Serrano (San Francisco: ASP), 283  
 Driver, S. P., Windhorst, R. A., Ostrander, E. J., Keel, W. C., Griffiths, R. E., & Ratnatunga, K. U. 1995, *ApJ*, 449, L23  
 Efstathiou, G., Bernstein, G., Katz, N., Tyson, J. A., & Guhathakurta, P. 1991, *ApJ*, 380, L47  
 Fomalont, E. B., Windhorst, R. A., Kristian, J. A., & Kellerman, K. I. 1991, *AJ*, 102, 1258  
 Forbes, D. A., Elson, R. A. W., Phillips, A. C., Koo, D. C., & Illingworth, G. D. 1994, *ApJ*, 437, L17  
 Forbes, D. A., Phillips, A. C., Koo, D. C., & Illingworth, G. D. 1996, *ApJ*, 462, 89  
 Glazebrook, K., Ellis, R., Colless, M., Broadhurst, T., Allington-Smith, J., & Tanvir, N. 1995a, *MNRAS*, 273, 157  
 Glazebrook, K., Ellis, R., Santiago, B., & Griffiths, R. 1995b, *MNRAS*, 275, L19  
 Griffiths, R. E., et al. 1994, *ApJ*, 437, 67  
 Gronwall, C., & Koo, D. C. 1995, *ApJ*, 440, L1  
 Groth, E. J., et al. 1996, in preparation  
 Guiderdoni, B., & Rocca-Volmerange, B. 1990, *A&A*, 227, 362  
 Guzmán, R., Koo, D. C., Faber, S. M., Illingworth, G. D., Takamiya, M., Kron, R. G., & Bershady, M. A. 1996, *ApJ*, 460, L5  
 Koo, D. C. 1995, in *Wide Field Spectroscopy and the Distant Universe*, ed. S. Maddox & A. Aragon-Salamanca (Singapore: World Scientific), 55  
 Koo, D. C., Guzmán, R., Faber, S. M., Illingworth, G. D., Bershady, M. A., Kron, R. G., & Takamiya, M. 1995, *ApJ*, 440, L49  
 Landy, S. D., Szalay, A. S., & Koo, D. C. 1996, *ApJ*, 460, 94  
 Le Fèvre, O., Crampton, D., Hammer, F., Lilly, S. J., & Tresse, L. 1994, *ApJ*, 423, L89  
 Lilly, S. J., Hammer, F., Le Fèvre, O., & Crampton, D. 1995a, *ApJ*, 455, 75  
 Lilly, S. J., Le Fèvre, O., Crampton, D., Hammer, F., & Tresse, L. 1995b, *ApJ*, 455, 50  
 Lilly, S. J., Tresse, L., Hammer, F., Le Fèvre, O., & Crampton, D. 1995c, *ApJ*, 455, 108  
 Majewski, S. R. 1993, *ARA&A*, 31, 575  
 McCarthy, P. J. 1993, *ARA&A*, 31, 639  
 McGaugh, S. S. 1994, *Nature*, 367, 538  
 Melnick, J. 1987, in *Starbursts and Galaxy Evolution*, ed. T. X. Thuan, T. Montmerle, & J. T. Thuan Van (Singapore: Edition Frontières), 215  
 Mould, J. 1993, in ASP Conf. Ser. 43, *Sky Surveys: Protostars to Protogalaxies*, ed. B. T. Soifer (San Francisco: ASP), 281  
 Oke, J. B., et al. 1995, *PASP*, 107, 375  
 Phillips, A. C., et al. 1996, in preparation  
 Ratnatunga, K. U., Ostrander, E. J., Griffiths, R. E., & Im, M. 1995, *ApJ*, 453, L5  
 Schade, D., Lilly, S. J., Crampton, D., Hammer, F., Le Fèvre, O., & Tresse, L. 1995, *ApJ*, 451, L1  
 Songaila, A., Cowie, L. L., Hu, E. M., & Gardner, J. P. 1994, *ApJS*, 94, 461  
 Steidel, C. C., Dickinson, M., & Persson, S. E. 1994, *ApJ*, 437, L75  
 Vogt, N. P., Forbes, A., Phillips, A. C., Gronwall, C., Faber, S. M., Illingworth, G. D., & Koo, D. C. 1996, *ApJ*, 465, L15